REPORT DOCUMENTATION PAGE

Form Approved
OMB NO. 0704-0188

1. AGENCY USE ONLY (Leave Blank)	2. REPORT DATE	3. REPORT TYPE AND DATES COVERED

4. TITLE AND SUBTITLE
An investigation of microstructure and grain boundary evolution during ECA pressing of pure aluminum

5. FUNDING NUMBERS

6. AUTHOR(S)
Terhune, Swisher, Oh-ishi, Horita, Langdon, McNelley

DAAD19-00-1-0488

7. PERFORMING ORGANIZATION NAME(S) AND ADDRESS(ES)
University of Southern California, Los Angeles, CA 90089-1453

8. PERFORMING ORGANIZATION REPORT NUMBER

9. SPONSORING / MONITORING AGENCY NAME(S) AND ADDRESS(ES)
U. S. Army Research Office
P.O. Box 12211
Research Triangle Park, NC 27709-2211

10. SPONSORING / MONITORING AGENCY REPORT NUMBER

40660.19-MS

11. SUPPLEMENTARY NOTES
The views, opinions and/or findings contained in this report are those of the author(s) and should not be construed as an official Department of the Army position, policy or decision, unless so designated by other documentation.

12 a. DISTRIBUTION / AVAILABILITY STATEMENT
Approved for public release; distribution unlimited.

13. ABSTRACT (Maximum 200 words)
This paper describes the microstructure in aluminum during ECAP.

14. SUBJECT TERMS	15. NUMBER OF PAGES
microstructure, ECAP	12
	16. PRICE CODE

17. SECURITY CLASSIFICATION OR REPORT	18. SECURITY CLASSIFICATION ON THIS PAGE	19. SECURITY CLASSIFICATION OF ABSTRACT	20. LIMITATION OF ABSTRACT
UNCLASSIFIED	UNCLASSIFIED	UNCLASSIFIED	UL

An Investigation of Microstructure and Grain-Boundary Evolution during ECA Pressing of Pure Aluminum

S.D. TERHUNE, D.L SWISHER, K. OH-ISHI, Z. HORITA, T.G. LANGDON, and T.R. McNELLEY

High-purity aluminum (99.99 pct) was processed by equal-channel angular pressing (ECAP) at room temperature through a die with a 90 deg angle between the die channels. Samples were examined by transmission electron microscopy (TEM) and orientation imaging microscopy (OIM) methods after one, four, and 12 passes through the die. Repetitively pressed samples were rotated by 90 deg in the same sense between successive pressing operations (route B_C). After one pressing, TEM showed a subgrain structure which was elongated in the shearing direction. Corresponding OIM data illustrated an inhomogeneous microstructure in which bandlike features were also aligned with the shearing direction. The lattice orientation varied from location to location in the material. The boundary disorientation distribution determined from the OIM data exhibited a peak at 2 to 5 deg, in agreement with a predominance of subgrains in the microstructure. After four pressings, the microstructure data obtained by TEM and OIM were mutually consistent. The disorientation data revealed a decrease in the population of 2 to 5 deg boundaries accompanied by an overall upward shift in the distribution. Two orientations were generally apparent in the texture, although specific orientations varied with location. Often, a ⟨111⟩ orientation tended to align with the shear direction. Following 12 ECA passes, the grain size was reduced further to about 1.0 μm. The populations of high-angle boundaries ($\geq$15 deg) increased in the disorientation distribution. A texture characteristic of shear deformation of fcc metals became apparent, although the orientations and particular components varied with location. Microstructural refinement during severe straining includes the development of large fractions of high-angle boundaries.

I. INTRODUCTION

THE properties of metallic materials may be improved through grain refinement using processes that include severe plastic deformation. Recent studies have shown that ultrafine grain sizes in the submicrometer or even nanometer range can be achieved by imposing extremely large plastic strains during deformation processing.[1–4] Methods such as high-pressure torsion loading,[1,5–8] high-energy ball milling,[9] sliding wear,[10] or equal-channel angular pressing (ECAP)[11–14] are required in order to impart strains which are sufficiently large to produce such grain refinement. During ECAP, a billet of material is pressed through a die having two channels, of equal cross section, which intersect at an angle; the arrangement of these channels is illustrated in the schematic of Figure 1 for a 90 deg die. Ideally, a billet experiences simple shear without any change in cross-sectional area upon passage through the intersection of the die channels, and the process is, therefore, amenable to repetition. For the coordinate axes shown in Figure 1, the billet is pressed downward in the $-z$ direction through the vertical channel and then exits the die in the $-x$ direction. The x, y, and z planes are the transverse, flow, and longitudinal planes, respectively, and the shape change in each of these planes is indicated in the insets in Figure 1 for a cubic element of material that is pressed through the die. The sense of the shear in the y plane is also illustrated in the inset at the lower-right-hand side.

Iwahashi *et al.*[13] have demonstrated that pure aluminum may be refined from an initial grain size of ~1.0 mm to an apparent grain size of ~1.3 μm after ECAP for four pressings at room temperature through a die with a 90 deg angle between the die channels. As successive pressings were performed, the microstructure evolved from one consisting of subgrains and low-angle boundaries to an apparently recrystallized state, with grains surrounded by high-angle boundaries. However, the conclusions regarding the grain boundaries were obtained by use of selected-area electron diffraction (SAED) methods in a transmission electron microscope. The SAED analysis used an aperture with a diameter of 12.3 μm, so that the diffraction data were simultaneously acquired from a large number of crystallites. Statistically significant grain-to-grain disorientation data can be acquired using recently developed orientation imaging microscopy (OIM) methods in a scanning electron microscope (SEM). The present investigation was, therefore, initiated in order to provide quantitative information on the evolution of the grain boundaries during repetitive ECAP of pure aluminum at room temperature. Here, the term "disorientation" refers to the minimum angle among all crystallographically equivalent rotations that bring the lattices of adjacent grains into coincidence.

Many factors affect the extent of grain refinement that

S.D. TERHUNE, formerly Graduate Student with the Department of Mechanical Engineering, Naval Postgraduate School, is with the United States Navy. D.L. SWISHER, Graduate Student, is with the Department of Mechanical Engineering, Naval Postgraduate School. K. OH-ISHI, Postdoctoral Research Associate, and Z. HORITA, Professor, are with the Department of Materials Science and Engineering, Kyushu University, Fukuoka, 812-8581, Japan. T.G. LANGDON, Professor, is with the Departments of Aerospace, Mechanical Engineering and Materials Science, University of Southern California, Los Angeles, CA 90089-1453. T.R. McNELLEY, Professor, is Chairman, Department of Mechanical Engineering, Naval Postgraduate School, Monterey, CA 93943-5146. Contact e-mail: tmcnelley@nps.navy. mil

Manuscript submitted July 6, 2001.

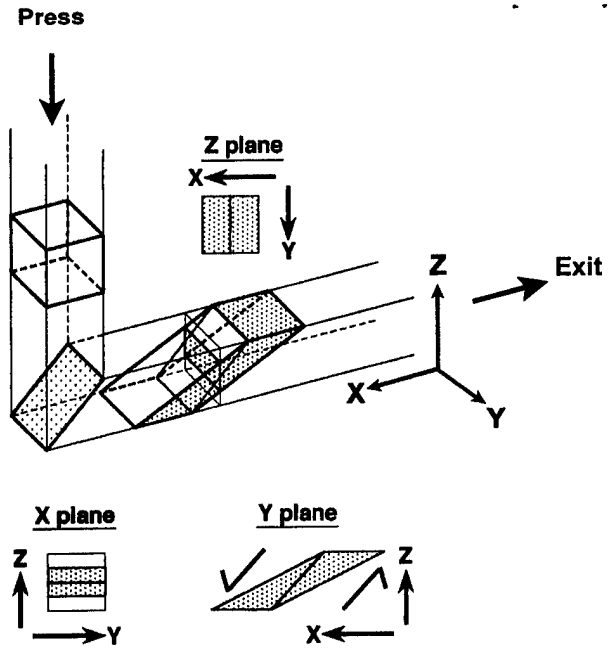

Fig. 1—A schematic representation of the channels in a 90 deg ECAP die. The coordinate axes that describe the x, y and z planes (or transverse, flow, and longitudinal planes, respectively) for as-pressed material are indicated. A sample billet, represented by the cubic element in the vertical channel, is pressed downward in the $-z$ direction through the channel intersection and exits the die in the $-x$ direction through the horizontal channel. For the cubic element, the shape changes in the x, y and z planes are illustrated in the insets. The sense of shear in the y plane upon passage through the channel intersection is also indicated.

results from processing by ECAP. Thus, further control of microstructural development during repetitive pressing may be obtained by rotation of the sample between successive passes through the die,[15] and several recent results have shown that different microstructural characteristics are obtained in pure aluminum, depending on the sequence of rotations between successive ECAP passes.[13,16,17] The relationship between the shear plane and shear direction on successive pressing operations depends upon the rotation between pressings. Four distinct procedures for repetitive pressings have been identified[18] and are illustrated in Figure 2. In route A, the sample is not rotated between successive passes. During pressing by route B, the sample may be rotated by 90 deg in an alternating sense (route B_A) or always in the same sense (route B_C). A fourth procedure involves rotation by 180 deg between successive passes (route C).

Following an initial ECAP pass, transmission electron microscopy (TEM) has revealed the presence of a cellular microstructure consisting of elongated, parallel bands of subgrains. These bands tend to be aligned with the top and bottom edges of the pressed sample (the y direction) when viewed in the x plane (Figure 1). They are also essentially parallel to the direction of shear in the y plane, which, in turn, is inclined at 45 deg to the top and bottom edges of the pressed sample (the x direction) when viewed in the y plane (Figure 1). In the z plane, the subgrain bands are arranged perpendicular to the direction of flow, which is the x direction. These microstructural features reflect the deformation occurring upon passage through the die, since this requires intense shear in the shear direction on a plane

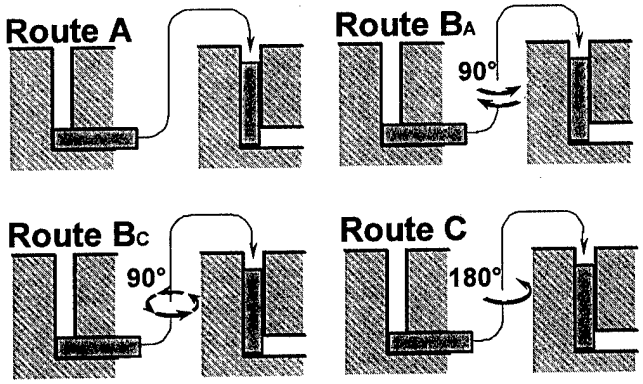

Fig. 2—Schematic illustrations of each of four processing routes for repetitive ECAP. In route A, the material is not rotated about its longitudinal axis between successive pressings; for route B_A, rotations are alternately +90 and −90 deg between successive passes. The rotation is always 90 deg in the same sense between passes in route B_C and 180 deg in the same sense for route C.

inclined at 45 deg to both x and z: this is the shaded plane defined by the intersection of the two die channels, as shown in Figure 1.

The shearing characteristics and the corresponding microstructural changes associated with the various possible processing routes have been analyzed for repetitive ECAP.[13,16] For pure aluminum processed using a 90 deg die, TEM data indicated that the evolution to a refined, equiaxed structure with an apparent presence of high-angle grain boundaries was most rapid for processing by route B_C, less rapid using route C, and slowest using routes A and B_A.[19] Subsequently, an interactive computer-aided electron-backscattered diffraction (EBSD) analysis method of acquiring grain-specific orientation data was employed to examine the evolution of the grain-to-grain disorientation-angle distribution during repetitive pressing of pure aluminum by route B_C.[20] A progressive increase in grain-boundary disorientation and randomization of the texture accompanied the refinement of the microstructure during repetitive ECAP. It was concluded that an ultrafine grain structure with high-angle boundaries had been achieved following 12 pressing passes, although the population of low-angle boundaries ($\leq$15 deg) remained greater than that expected from texture considerations. This reflected the deformation-induced boundaries associated with each successive pressing operation.[20]

The use of automated OIM allows imaging of the microstructure based on the orientation measurements, as well as the presentation of microtexture and grain-boundary data. In the following sections, TEM results and the corresponding OIM data are presented for material after one ECAP pass and for samples repetitively pressed through four or 12 passes using route B_C.

II. EXPERIMENTAL PROCEDURES

A. *Material and Procedure for ECAP*

The material used in this study was commercially available pure (99.99 pct) ingot-metallurgy aluminum. The as-received material was rolled into a plate at room temperature and cut to provide billets with dimensions of 25 × 25 × 150 mm^3. These billets were swaged at room temperature

to rods of 10 mm in diameter, which were cut into lengths of ~60 mm and then annealed for 1 hour at 550 °C. Optical microscopy revealed a recrystallized grain size of ~1 mm. Laue X-ray data indicated that there was no discernable preferred orientation in this coarse-grained material, although recent neutron-diffraction experiments have suggested that there is a weak tendency for a ⟨111⟩ orientation to align with the axis of the swaged rods in a partial fiber texture.[21] The ECAP die channel was of circular cross section, with a diameter of 10 mm. Using the notation of Iwahashi *et al.*,[22] the internal angle (Φ) between the die channels was 90 deg, and the angle (Ψ) subtended by the outer arc of curvature at the intersection between the two channel sections was 20 deg. For each pass through a die with a square configuration ($\Psi = 0$ deg), the equivalent strain was $\epsilon_{eq} = 1.15$; this is an upper bound for the strain, and the introduction of an outer arc of curvature at the intersection of the die channels results in an equivalent strain for a pass that is less than this value. When $\Psi = 20$ deg $\epsilon_{eq} \sim 1.0$, giving a total strain accumulation of N_p, where N_p is the number of passes through the die.[22] Finite-element analysis of billet deformation during ECAP has shown that the deformation is more complex than simple shear on the plane formed by the intersection of the die channels. Instead, straining occurs along an arc as the billet passes through the intersection of the die channels. Die-wall friction and strain hardening of the material influence the strain distribution in the billet as well as the details of the die geometry and the processing route.[23,24]

In the present work, pressing was carried out at room temperature (25 °C) by placing a sample in the vertical section of the die channel and then pressing through the die with a plunger at a speed of 19 mm s^{-1}. Recent measurements have shown that the temperature rises to about 40 °C in a time interval of about 1 second during pressing at this speed, but thereafter, the temperature decreases to ambient in about 60 seconds after completion of ECAP.[25] The samples examined in this study were pressed one, four, or 12 times with approximate total accumulated strains of ~1, ~4, or ~12, respectively. Repetitive pressings were performed following route B_C (Figure 2). Examination of Figure 1 reveals that the orientation of the shear direction will differ by 90 deg when comparing a plane whose normal is the $+y$ direction to one with the $-y$ direction as its normal, and this distinction is especially important in the interpretation of texture data.

B. *The TEM Examination*

Samples were prepared as thin foils for examination in the as-pressed condition. All of these samples were sectioned so that the foil normal was parallel to the y direction (*i.e.*, the foils were parallel to the y, or flow, plane). Accordingly, the first sectioning was perpendicular to the axis of the pressed samples, and these samples were subsequently sectioned parallel to the y plane to provide a slice approximately 0.5 mm in thickness. Disks were sectioned from these slices with a diameter of 3 mm and then ground to a thickness of about 0.15 mm. The disks were thinned to perforation for TEM examination using a twin-jet electropolishing technique with a solution of 10 pct $HClO_4$ + 20 pct CH_3OH + 70 pct C_2H_5OH at a temperature of about 5 °C. Microstructural observations were made using an Hitachi H-8100 transmission electron microscope operating at 200 kV. Representative photomicrographs were obtained to determine the subgrain or grain size using the mean linear-intercept method. The SAED patterns were acquired using an aperture of 12.3 μm in diameter in order to assess the spread of orientations within each region.

C. *The OIM Examination*

Samples were examined on a plane containing the centerline of the as-pressed material and having its normal lying parallel to the $-y$ direction (Figure 1). The electron beam of the SEM (Topcon SM-510) is used as an orientation probe during OIM. The SEM was operated at 20 kV with a beam-spot diameter of approximately 40 nm, and so the electrons interact within about 50 nm of the sample surface to produce diffraction patterns. This requires that the residual strains due to sample preparation be minimized. Accordingly, samples were mechanically polished with a succession of abrasives which concluded with colloidal silica. Final electropolishing was accomplished at 35 V for 20 to 30 seconds using a 20 pct $HClO_4$ + 80 pct C_2H_5OH solution cooled to −25 °C.

In order to accomplish OIM, the electron beam is deflected, point by point, in a raster on the sample surface. At each point in the raster, the EBSD results in the formation of Kikuchi patterns on a phosphor screen in the SEM chamber. A thorough background on EBSD and the data acquisition and analysis procedures relevant to OIM have been provided by Randle.[26] The Kikuchi patterns are recorded by a low-light camera, captured by system software (EDAX/TSL, Inc.), and then analyzed and indexed as the Euler angles ϕ_1, Φ, and ϕ_2, which specify the orientation of the lattice relative to a reference frame defined by the sample stage. The angles and the corresponding location on the sample surface are then stored. The Kikuchi patterns obtained in this manner allow an unambiguous determination of the lattice orientation. The point-to-point distance, or step size, was based on the expected microstructure and size of the region investigated. Typically, areas 20 × 20 μm in size were examined using a step distance between successive points of 0.2 μm, although data acquisition for the purpose of texture analysis often involved larger areas and step sizes.

Data cleanup procedures were used to ensure that data points with a probability ≥95 pct of correct indexing were retained for subsequent analysis. Individual points having a lower probability of correct automatic indexing were assigned to neighboring regions of similar orientation. Two factors generally resulted in a low probability of correct indexing. These were, first, the overlapping of diffraction patterns when the beam was positioned nearby a grain boundary, and second, pattern degradation due to high local lattice strain, which was also most apparent in the vicinity of boundaries. Several methods of OIM data representation were employed. Color-coded grain-orientation maps were produced by assigning data points to the same grain if neighboring lattice orientations differed by less than 2 deg. Discrete pole figures were employed to examine the microtexture corresponding to the region investigated. Histograms were produced to assess the distribution of grain-to-grain disorientation angles; the data were always grouped into 13 bins, each 5 deg in width. There are two main sources of error in the disorientation data. The first is a standard error due to the number of disorientations in a data set, *i.e.*,

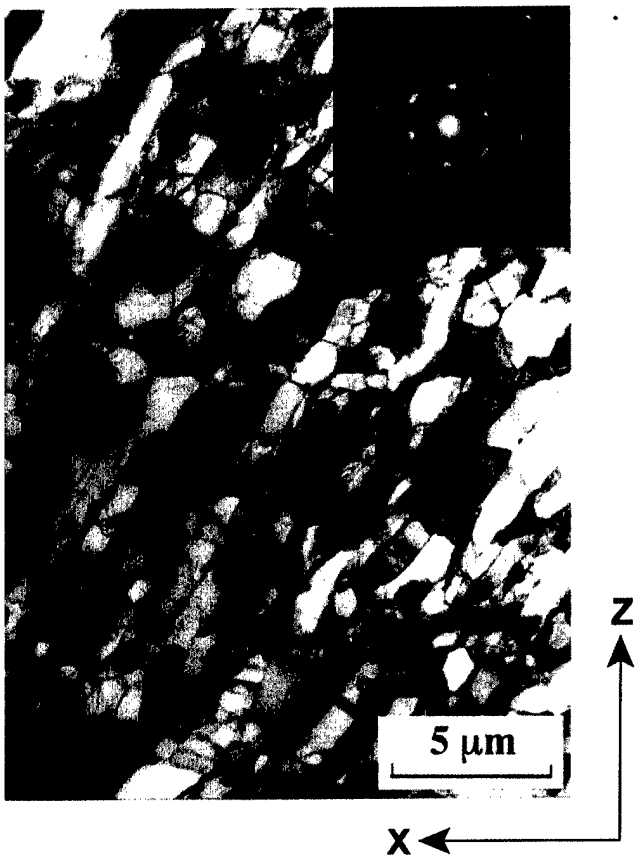

Fig. 3—A bright-field transmission electron micrograph and SAED pattern showing a representative microstructure in the y plane for pure aluminum after one pressing pass. The subgrain bands are aligned with the shear direction (Fig. 1). The SAED pattern was obtained for a region 12.3 μm in diameter.

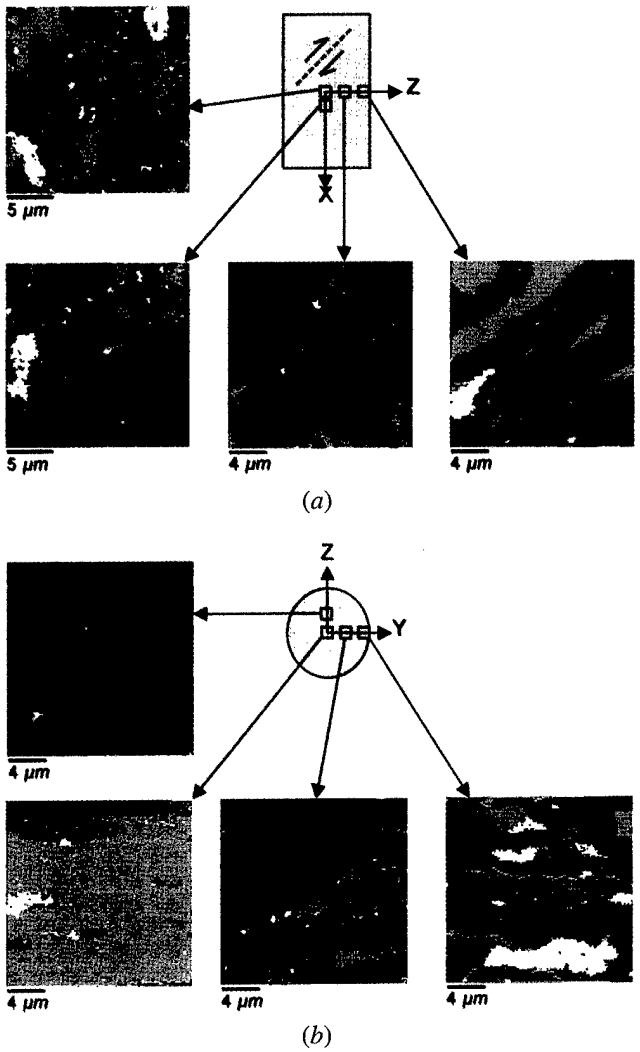

Fig. 4—Grain maps obtained by OIM of pure aluminum processed by one ECAP pass showing an inhomogeneous microstructure. Different colors correspond to orientations differing by more than 2 deg. (*a*) The relative locations on the y plane of these 20 μm × 20 μm maps are indicated by the inset schematic of a sample that has been sectioned to reveal this plane. (*b*) The relative locations on the x plane of the maps are also indicated by the inset schematic of a sample that has been sectioned to reveal the x plane.

$SE_N = \sqrt{x_i(1 - x_i)/N}$, where SE_N is the standard error due to the size of the data set, N is the number of disorientations in the data set, and x_i is the fraction of N that is contained in the ith bin of the disorientation distribution. The second is a standard error due to the resolution limit for disorientation determination in the software, *i.e.*, $SE_\theta = \theta_{\text{resolution}}/\theta_{\max}$, where $\theta_{\text{resolution}} = 2$ deg and $\theta_{\max} = 62.8$, *i.e.*, the maximum possible disorientation considering all crystallographically equivalent rotations bringing adjacent lattices into coincidence. Then, the total standard error is $SE_{\text{tot}} = \sqrt{(SE_N)^2 + (SE_\theta)^2}$. In the present work, $N \geq 2000$ for all materials following ECAP and so, $SE_{\text{tot}} \approx SE_\theta = 0.032$. The histograms were converted to probability density distributions; in this form, $SE_{\text{tot}} \approx 0.006$. Smooth curves were then fit to the data for material processed by four or 12 ECAP passes.

III. RESULTS

A. *One ECAP Pass*

The microstructure in the y plane of this material after one ECAP pass is shown in the TEM micrograph in Figure 3. The orientation of the micrograph relative to the x and z-axes of the as-pressed sample is shown in the inset. It is apparent that this structure consists of bands of elongated (sub)grains that are approximately aligned in the shear direction; the SAED pattern suggests that the subgrains are of relatively low disorientation. Iwahashi *et al.*[13] have shown that these bands also extend along the y direction in both the x and the z planes, so that these bands are slablike and elongated in the shear direction on the shear plane. The (sub)grains within the bands are also elongated in the shear direction and aligned with the shear plane. Mean linear-intercept measurements from these micrographs show that the subgrains are about 4 μm in length along the shear direction and about 1.2 μm in thickness when measured along the shear plane normal.

Results of OIM analysis of this material after one ECAP pass are presented in Figure 4, which shows grain-color maps obtained at various locations on the y plane (Figure 4(a)) as well as on the x plane (Figure 4(b)). The schematic diagrams of the y and x planes in sectioned samples show the approximate locations from which these images were obtained. Different colors in these maps correspond to neighboring orientations that differ by more than 2 deg;

thus, these data indicate a distinctly inhomogeneous microstructure at this resolution of orientation. The maps obtained on the y plane display bandlike features, although the apparent width of the bands varies from about 1.0 μm to more than 10 μm. In Figure 4(a), these bands have the appearance of elongated grains at the location along the z-axis nearest to the sample surface. The normal to all of the maps in Figure 4(a) is the $+y$ direction, while the corresponding normal to the TEM micrograph of Figure 3 is the $-y$ direction. Thus, the bands in both Figures 3 and 4(a) exhibit essentially the same inclination to the x- and z-axes. A comparison of TEM and OIM results suggests that the bandlike features evident in the OIM data of Figure 4(a) are further divided into bands of elongated subgrains of a disorientation <2 deg.

An inhomogeneous microstructure is also evident in the x plane (Figure 4(b)). The bands now extend along the y direction, which corresponds to the trace of the shear plane, although the width of the bands when measured along the z direction apparently exceeds 20 μm in some locations. These results are in general agreement with those of Iwahashi *et al.*[13] and also suggest a structure that comprises slablike bands that lie on the shear plane and which are elongated in the shear direction. From TEM, a subgrain structure is located within these bands.

Discrete pole figures corresponding to the data of Figure 4 are presented in Figure 5. These data were all acquired at the middle of the y plane, but from regions of varying size. The step sizes were varied as well, and the relative sizes of the regions from which these data were acquired are illustrated schematically along with the (200), (220), and (111) discrete pole figures. These data are also consistent with an inhomogeneous microstructure following one ECAP pass. The data acquired from an area 20 × 20 μm in size (Figure 5(a)) show a single predominant orientation. Examination of the (111) discrete pole figure in Figure 5(a) reveals that a ⟨111⟩ orientation lies in the shear plane and is rotated approximately 20 deg away from the shear direction toward the y-axis. Data from an area 100 × 100 μm in size are shown in Figure 5(b); this region includes the smaller area of the data of Figure 5(a). Several distinct orientations are apparent in this larger region, although another area of the same 100 × 100 μm size (Figure 5(c)) exhibits only a single predominant orientation. A ⟨111⟩ orientation is aligned with the shear direction in the region of Figure 5(c).

The scatter about the predominant orientation(s) in the discrete pole figures of Figure 5 also suggests the presence of a large population of low-angle boundaries, and this is shown in the disorientation distributions shown in Figure 6. Data from three locations distributed along the z-axis on the y plane are shown in Figure 6(a). In all cases, about 50 pct of the boundaries are of a 2 to 5 deg disorientation, *i.e*, the structure is mainly made up of subgrains after one ECAP pass. There also appear to be peaks in these distributions near 30 deg and between 55 and 60 deg of disorientation. The populations in these distributions generally differ by more than the standard error in the data, and, thus, the disorientation distribution is not uniform after one ECAP pass. This is also the case for data acquired on the x plane from various locations along either the y- or the z-axes, as shown in Figure 6(b). Peaks in these distributions at 30 to

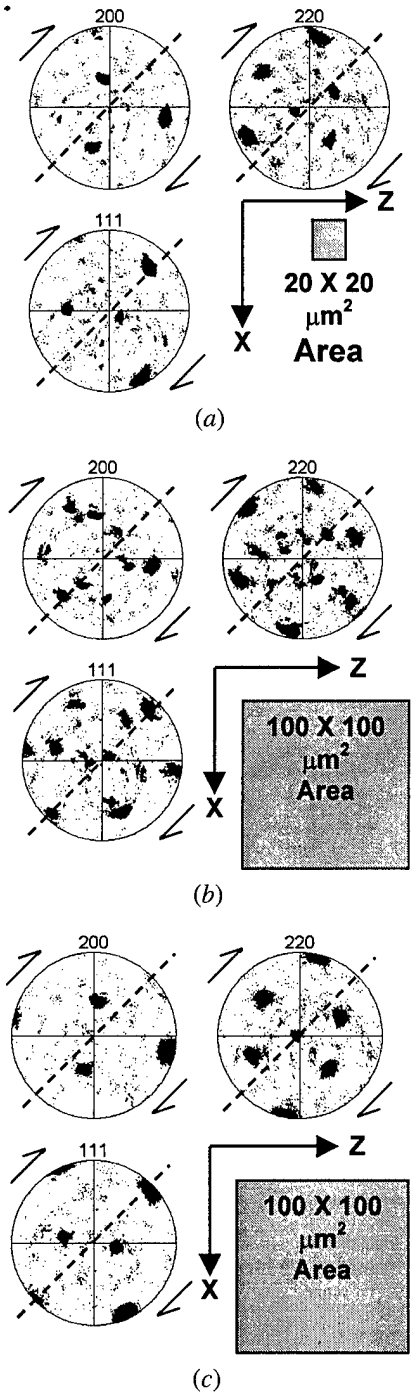

Fig. 5—Representative discrete pole figures from regions located near the center of the y plane showing the microtexture of pure aluminum after one ECAP pass. The diagonal dashed lines represent the shear plane trace, while the arrows illustrate the sense of the shear. (*a*) There is a single orientation within a small (20 μm × 20 μm) region. (*b*) Multiple orientations within a larger (100 μm × 100 μm) region that contains the area of (a). (*c*) The ⟨111⟩ is aligned with the shear direction in a nearby region near the center of the y plane.

40 deg are especially prominent in data at the center of the x plane and at the half-radius along the y direction. Comparison of the distribution in Figures 6(a) and (b) suggests that the population of low-angle (2 to 5 deg) boundaries is relatively lower on the x plane than on the y plane, and that the disorientation distribution depends on the plane

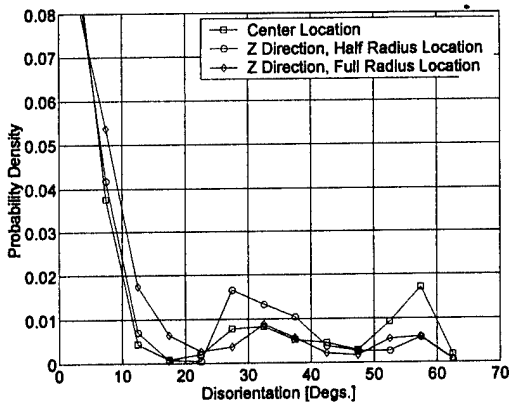

(*a*)

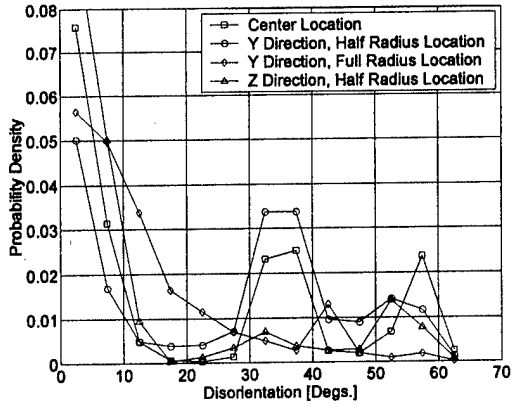

(*b*)

Fig. 6—The probability density distributions of boundaries as a function of disorientation angle for pure aluminum after one ECAP pass. These data are consistent with an inhomogeneous microstructure. (*a*) Data from various locations in the *y* plane, which correspond to the locations indicated in the schematic inset in Fig. 4(a). (*b*) Data from various locations on the *x* plane are shown; these locations correspond to the schematic inset in Fig. 4(b).

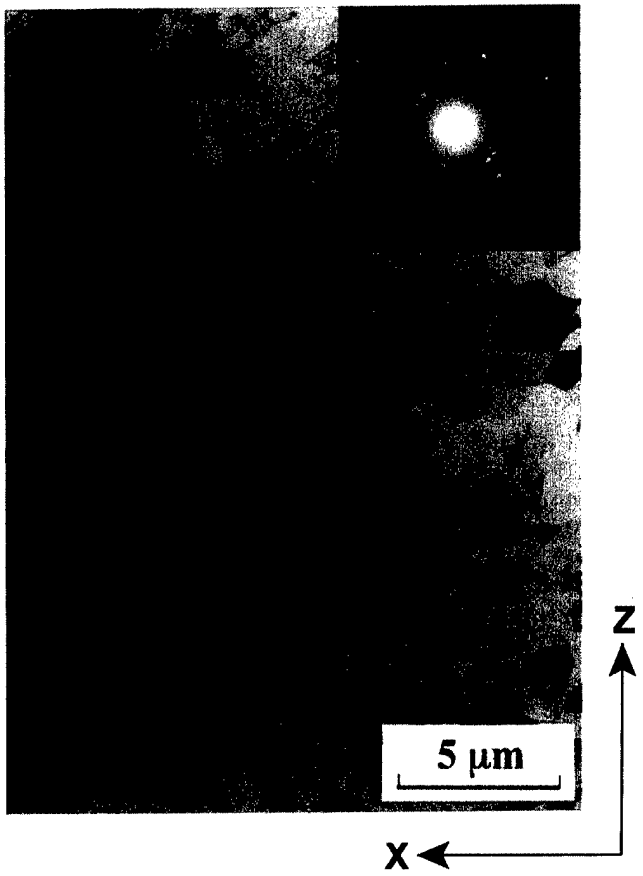

Fig. 7—A bright-field transmission electron micrograph and SAED pattern showing a representative microstructure in the *y* plane for pure aluminum after four pressing passes by route B_C. The sample orientation is the same as in Fig. 3. The SAED pattern was also obtained for a region 12.3 μm in diameter.

of observation, *i.e.*, the distribution is not isotropic in nature.

B. *Four ECAP Passes by Route B_C*

Figure 7 is a TEM micrograph in the *y* plane for a sample examined after four ECAP passes by route B_C. The orientation of the micrograph relative to the axes of the as-pressed condition is shown in the inset; these axes pertain to the final (fourth) pressing pass. A nearly equiaxed (sub)grain structure has replaced the bandlike substructure formed in the initial pressing operation, although careful examination of Figure 7 reveals a tendency for the (sub)grains to align in the shear direction of the final pressing pass. A mean linear-intercept value of 1.2 μm was obtained for this microstructure, and the SAED pattern suggests a larger spread in orientation among the (sub)grains than is apparent after the initial pressing pass (Figure 3).

The grain-color maps obtained by OIM after four ECAP passes by route B_C are shown in Figure 8, which includes maps from various locations on the *y* plane (Figure 8(a)) as well as on the *x* plane (Figure 8(b)). Again, different colors in these maps are used to distinguish neighboring orientations that differ by more than 2 deg. Mean linear-intercept values of 1.2 to 1.4 μm were obtained from these grain maps, which is generally consistent with the results of TEM for this same condition. Repetitive ECAP has produced a much more homogeneous microstructure at this level of orientation resolution, as revealed by comparison with the maps in Figure 4 for this material after one pass. However, alignment of the (sub)grains with the shear direction is also apparent in all of the images from the *y* plane in Figure 8(a). Furthermore, in some regions of these maps, the (sub)grains appear to be organized into bands of about 8 μm in thickness when measured along the normal to the shear plane, which are also aligned with the shear direction. The microstructure exhibits little variation from location to location on either the *y* plane or the *x* plane (Figure 8(b)). The apparent grain shape in the *x* plane is irregular, and the bandlike arrangement of the (sub)grains noted in the *y* plane cannot be readily discerned in this plane.

Microtexture data in the form of discrete pole figures were similar for the various regions examined, although small (20 × 20 μm) regions often exhibited a single orientation while larger (100 × 100 μm) regions exhibited multiple orientations. A representative example of the microtexture is shown in Figure 9(a); these data were obtained from an area 100 × 100 μm in size that was located at the center of the *y* plane. Inspection of these discrete pole figures reveals that there are two prominent orientations in the material. The scatter in these orientations is consistent with the

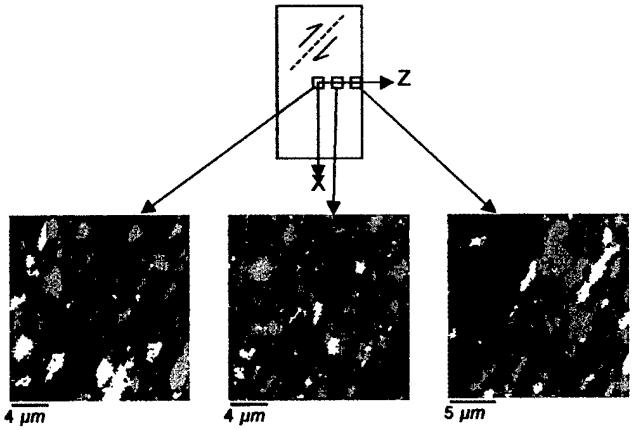

(*a*)

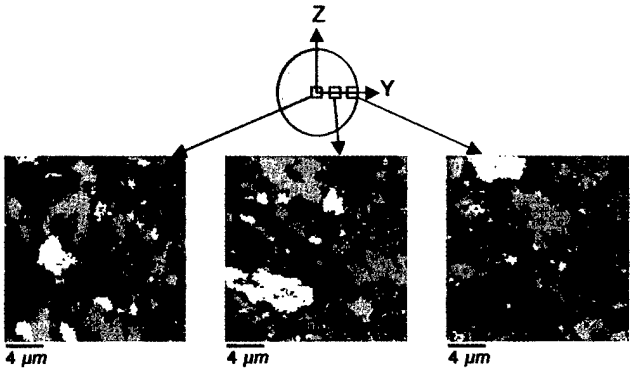

(*b*)

Fig. 8—Grain maps produced by OIM analysis of pure aluminum following four ECAP passes by route B_C, showing that a more homogeneous microstructure has been achieved after four pressing operations. (*a*) The 20 μm × 20 μm maps and their relative locations on the *y* plane are shown. (*b*) The maps and their locations on the *x* plane are indicated.

presence of low-angle boundaries, and this is also apparent in the disorientation distributions shown in Figures 9(b) and (c). These data were acquired from various locations on either the *y* (Figure 9(b)) or the *x* (Figure 9(c)) planes. Within the uncertainty of measurement, the data from the various locations on either plane are identical, which is consistent with the observation of a homogeneous microstructure after four ECAP passes. In both cases, the population of low-angle (2 to 5 deg) boundaries has been reduced after four passes, in comparison to material processed through only an initial pass. Overall, the data for one and four passes indicate that repetitive ECAP results in an upward shift in the distribution of boundary disorientations. However, the data obtained on the *x* plane show distinctly larger populations of boundaries of either a 30 to 40 deg or 55 to 62.8 deg disorientation than that obtained on the *y* plane, and so the disorientation distribution remains anisotropic in nature.

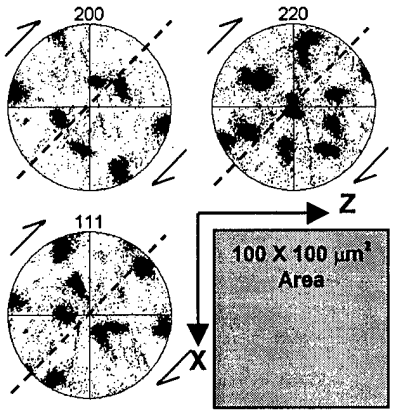

(*a*)

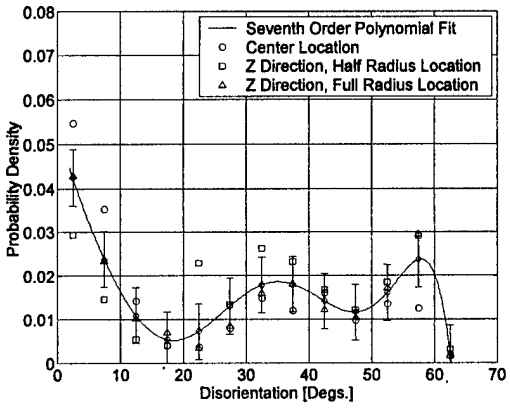

(*b*)

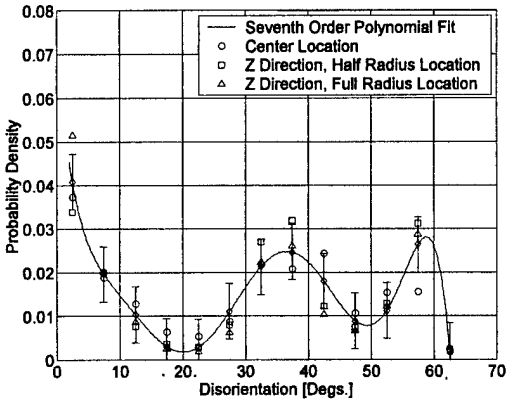

(*c*)

Fig. 9—(*a*) A representative discrete pole figure obtained near the center of the *y* plane for pure aluminum following four ECAP passes by route B_C. The diagonal dashed lines represent the shear plane trace, while the arrows illustrate the sense of the shear; two distinct orientations are evident and a ⟨111⟩ tends to be aligned with the shear direction. The probability density distributions of boundaries as functions of disorientation angle for pure aluminum after four passes are shown (*b*) for the *y* plane and (*c*) for the *x* plane. The error bars correspond to the total standard error.

C. *Twelve ECAP Passes by Route B_C*

The microstructure in the *y* plane following 12 ECAP passes by route B_C is shown in Figure 10. A mean linear-intercept value of 1.0 μm for this condition suggests that further, gradual refinement of the microstructure took place during the eight repetitive ECAP passes following the condition shown in Figure 7. The structure is similar to that obtained after four passes by route B_C, in that nearly equiaxed (sub)grains still exhibit a tendency to align along the shear plane in the shearing direction of the final pass. Well-defined boundaries are apparent in Figure 10, and the (sub)-grain interiors are largely free of dislocations. The SAED pattern illustrates a large spread in orientations in this microstructure.

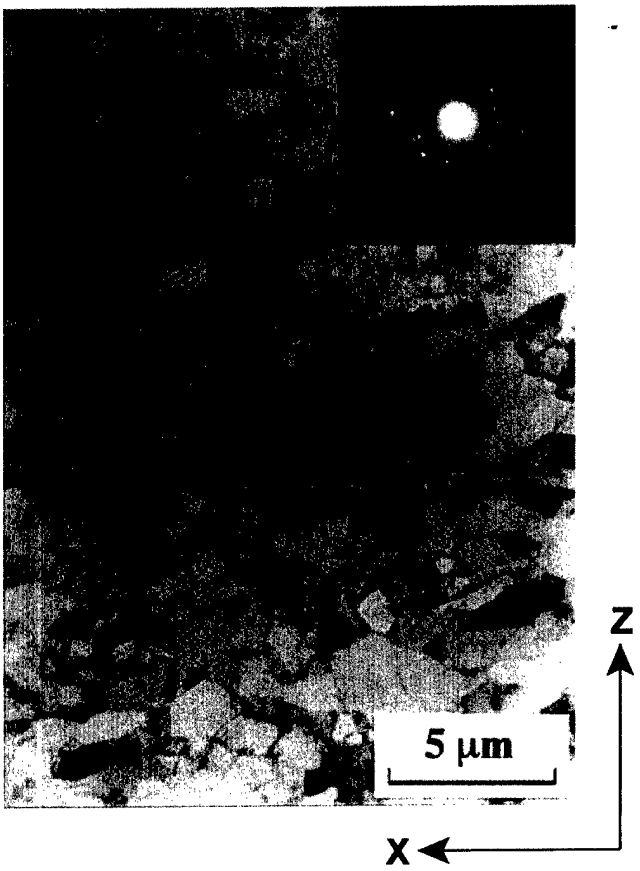

Fig. 10—A bright-field transmission electron micrograph and SAED pattern showing a representative microstructure in the *y* plane for pure aluminum after 12 pressing passes by route B_C. The sample orientation is again the same as in Figs. 3 and 7. The SAED pattern was also obtained for a region 12.3 μm in diameter.

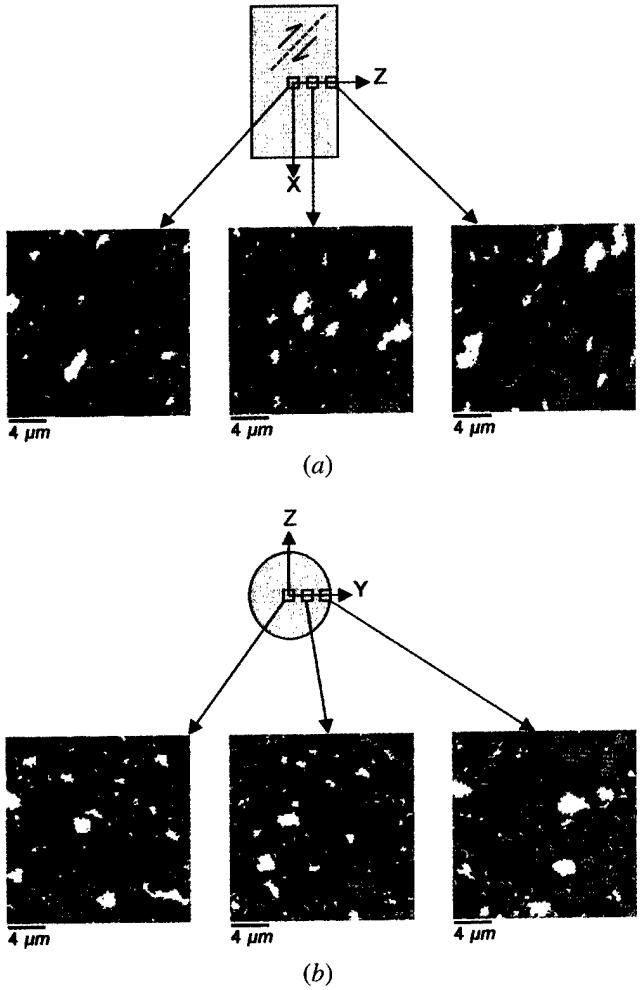

Fig. 11—Grain maps of pure aluminum produced by OIM analysis of pure aluminum pressed 12 times by route B_C. (*a*) The 20 μm × 20 μm maps and their relative locations on the *y* plane. (*b*) The maps and their locations on the *x* plane are indicated. These maps demonstrate the achievement of a uniform and homogeneous microstructure by ECAP.

The OIM grain-color maps in Figure 11 illustrate a homogeneous as well as highly refined microstructure after 12 ECAP passes by route B_C. A mean linear-intercept value of 1.0 μm was obtained from these maps, which is identical to the result obtained in TEM. This suggests that OIM is resolving essentially all of the grains that are present in material processed to this condition. A tendency in the structure to align with the shear direction is evident in all of the locations examined on the *y* plane (Figure 11(a)), but further organization of the (sub)grains into bands is not apparent in these maps. The irregularly shaped (sub)grains observed in the *x* plane after four ECAP passes (Figure 8(b)) have been replaced by a refined, equiaxed structure after 12 ECAP passes, as illustrated in Figure 11(b). There is a tendency for these (sub)grains to align with the *y*-axis in the *x* plane, which is parallel to the trace of the shear plane.

Following 12 ECAP passes, the discrete pole-figure data were also consistent with homogenization of the structure. A representative example of the microtexture is shown in Figure 12(a) for an area 100 × 100 μm in size that is located at the center of the *y* plane. This is a shear texture for an fcc metal; using the nomenclature introduced by Canova *et al.*,[27] this is a B-type shear texture in which a ⟨110⟩ orientation tends to align with the shear direction. The B-type shear-texture component exhibits rotational symmetry about the shear direction, and this may be seen in all three discrete pole figures, *e.g.*, as the band of orientations perpendicular to the shear direction in the (111) discrete pole figure. Corresponding disorientation distributions are included in Figure 12(b) for the *y* plane and in Figure 12(c) for the *x* plane. The disorientation data are consistent with homogenization of the microstructure, but the distribution is still anisotropic in nature. In both the *y* plane and the *x* plane, the populations of low-angle boundaries (2 to 5 deg) have been further reduced following 12 repetitive ECAP passes when compared to the data for four passes. Thus, there has been a further upward shift in the distribution of boundary disorientations. The data obtained on the *x* plane still show distinctly larger populations of 30 to 40 deg and 55 to 62.8 deg boundaries than the data for the *y* plane.

IV. DISCUSSION

A. *The current investigation*

It is now well established that severe plastic deformation by repetitive ECAP may be employed to produce ultrafine

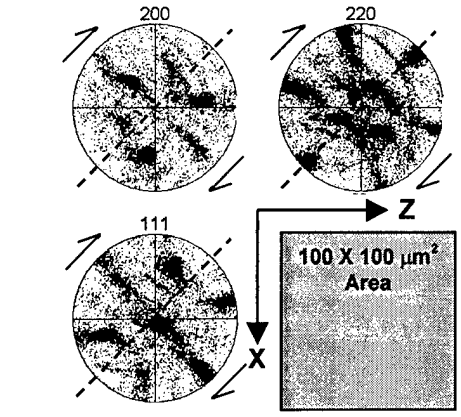

(*a*)

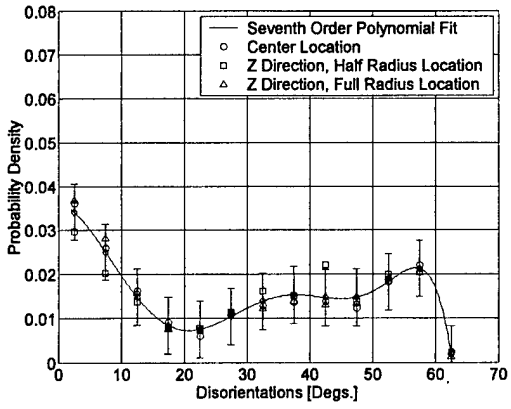

(*b*)

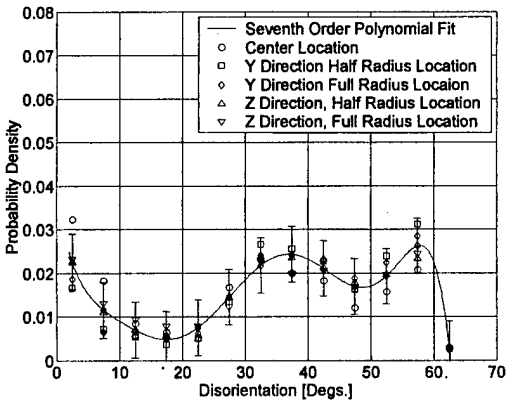

(*c*)

Fig. 12—(*a*) A representative discrete pole figure for pure aluminum following 12 ECAP passes by route B_C. These data were obtained from the *x* plane and the axes were subsequently rotated to correspond to the *y* face. The diagonal dashed lines represent the shear plane trace, while the arrows illustrate the sense of the shear. A B-type shear texture has formed after 12 ECAP passes by route B_C.[27] The probability density distributions of boundaries as functions of disorientation angle for pure aluminum after 12 passes are shown (*b*) for the *y* plane and (*c*) for the *x* plane. The error bars correspond to the total standard error.

grain sizes in polycrystalline materials. However, predictive models for the process of grain refinement remain to be developed. Processing of pure aluminum with an initial grain size of about 1.0 mm through a single ECAP operation at room temperature leads to the development of elongated bands of subgrains. From TEM results, the subgrains have lengths of about 4.0 μm along the shear direction and widths of about 1.2 μm along the shear plane normal. A banded microstructure is also evident in the OIM results following one ECAP pass, but the widths of the bands are not uniform and lattice orientations are not homogeneous throughout the structure. The microtexture varies with location as well as with the size of regions examined. The disorientation distributions obtained from OIM are consistent with a predominance of subgrains in the microstructure. However, comparison of TEM micrographs and OIM grain maps for material processed through one ECAP pass clearly indicates that the 2 deg limit on the resolution of a disorientation leaves out many boundaries of disorientation below this resolution limit. The disorientation data are anisotropic; no more than 20 pct of the boundaries on the *y* plane are >15 deg in disorientation, and the corresponding value on the *x* plane is 40 pct > 15 deg. The inhomogeneous nature of the band structure and the microtexture reflects a coarse initial grain size and inhomogeneous deformation due to differences in initial orientations of the grains prior to the first ECAP pressing operation.

Several earlier observations have led to the conclusion that it is advantageous to rotate the sample billet between successive ECAP operations. In the present experiments, a refined and nearly equiaxed grain structure was present following four successive ECAP passes by route B_C, and similar microstructural results were obtained by both TEM and OIM analysis. The microtexture results from OIM analysis are consistent with a more homogeneous microstructure. However, careful examination of the microstructures revealed by both methods of analysis indicate that the (sub)grains on the *y* plane are aligned in bands that are parallel to the shear direction. At this point in the processing, a mean linear-intercept value of about 1.2 μm may be obtained from TEM data, and a corresponding mean linear-intercept value of 1.2 to 1.4 μm may be obtained from the OIM data. Thus, fewer boundaries are remaining undetected in the OIM analysis. Again, the boundary disorientation distributions were different on the *y* and *x* planes, but were consistently independent of location on each of these planes, and this is also indicative that the microstructure was homogenized by four ECAP passes. Comparison of the disorientations after one and four passes reveals that the distribution has shifted upward in angle following four successive ECAP operations by route B_C. After four passes, 60 pct of the boundaries have a disorientation >15 deg on the *y* plane, while 65 pct have a disorientation >15 deg on the *x* plane. The increase in disorientation during repetitive pressing reflects the accumulation of dislocations into the (sub)grain boundary walls *via* recovery processes during straining, and this same conclusion was reached in the earlier study which employed an interactive EBSD method to acquire grain-orientation data.[20] Chang *et al.*[28] also reached a similar conclusion based on disorientation measurements during TEM investigation of pure aluminum which had been processed by ECAP to strains of ~2, ~4, or ~8 following route B_C.

In the current study, both TEM and OIM revealed a further small reduction in the grain size to about 1.0 μm, associated with straining beyond four ECAP passes *via* route B_C. However, the OIM data indicated that large changes in the texture had occurred during these additional ECAP passes, and that

a B-type shear texture had developed in material processed by 12 ECAP passes *via* route B_C. Following Canova *et al.*,[27] the B-type shear texture may be denoted as {hkl} ⟨110⟩, wherein the {hk} pole refers to the lattice plane parallel to the shear plane and ⟨110⟩ is the direction parallel to the shear direction, *i.e.*, it is a fiber texture having the shear direction as the fiber axis. The shear direction is denoted by the dashed line in Figure 12(a), and rotational symmetry about the shear direction is evident in all of the pole figures for this processing condition. However, the distribution about the fiber axis is nonuniform. Furthermore, some variation of texture with location was still noted in samples that had been processed by 12 ECAP passes with route B_C. In the example shown in Figure 12(a), there appears to be a prominent orientation that has a ⟨111⟩ orientation aligned near the *y* direction.

After one ECAP, the texture varied greatly with location. Also, none of the orientations associated with shear textures were apparent after four ECAP passes by route B_C. Thus, the B-type shear texture observed after 12 ECAP passes by route B_C developed during repetitive pressing after the fourth ECAP pass. Models of texture evolution for simple shear deformation under torsion of a material having initially random lattice orientations indicate that shear-texture components would be expected to develop gradually over increasing strains. For example, Canova *et al.*[27] showed that both A-type ({111}⟨hkl⟩) and B-type shear-texture components initially formed in a material of random initial texture, and, for conditions of relaxed constraints, a stable B-type texture became predominant. Models to describe texture evolution during repetitive ECAP, including dependence on processing route, remain to be developed.

The disorientation distribution of an ideal fiber texture would be a line at a constant probability density of ≈0.015 in Figures 12(b) and (c). However, a significant population of random orientations is evident following 12 ECAP passes by route B_C. Thus, the disorientation distribution consists of a population of boundaries associated with the shear texture, a population of boundaries associated with the random component, and low-angle boundaries likely introduced in the final pressing pass. From the distributions for this material following 12 ECAP passes, 63 pct of the boundaries have a disorientation >15 deg in the *y* plane, and 78 pct have a disorientation >15 deg in the *x* plane. The progressive increase in boundary disorientation during repetitive ECAP by route B_C is summarized in Figure 13 as the fraction of high-angle boundaries (disorientation >15 deg) as a function of the number of ECAP passes. In this form, these data clearly show an increase in the population of high-angle boundaries associated with repetitive ECAP operations. These data agree with the results of Chang *et al.*,[29] who showed a similar, rapid increase in the population of high-angle boundaries during the first four passes and a subsequent, more gradual increase beyond four passes in repetitive ECAP. Qualitatively, the same trend was also observed in an earlier investigation[20] using an interactive EBSD method. After one pass, the boundaries were predominantly low-angle boundaries in character, and the population of high-angle boundaries had increased in material following four ECAP passes by route B_C. A texture was apparent in both cases. However, material processed through 12 ECAP passes by route B_C exhibited a random texture, and the corresponding disorientation distribution was close to the Mackenzie random distribution.[30] While this reflected a further increase in the population of high-angle boundaries,[20] the appearance of a random texture after 12 ECAP passes may reflect the onset of recrystallization, which evidently did not occur in the material and processing of the current study. Differences in the details of either the composition or the processing may account for such a difference in behavior.

Anisotropy in the disorientation distribution has been reported in a study of the grain boundaries in Supral 2004, a superplastic aluminum alloy which exhibited a banded deformation-induced microstructure.[31] A model was proposed that assumed that the interfaces between such bands were the high-angle boundaries, and the low-angle boundaries then separated cells in a cellular substructure within the bands. It was shown that such a banded structure will result in different relative populations of high-angle and low-angle boundaries on different planes of observation. The microstructures observed here in material following one or four ECAP passes show bandlike features, and it is deemed likely that such bands may account for the differences in the disorientation distributions on the *y* and *x* planes in the present investigation.

B. *Relevance of these Results to Other Investigations*

In several earlier reports on microstructural development in ECAP, the disorientations of the boundaries introduced through pressing were inferred indirectly from careful examination of SAED patterns.[13,16] However, this procedure yields only qualitative information on the nature of the disorientations, and it is necessary in practice to use more sophisticated techniques such as EBSD or analysis of Kikuchi patterns in TEM[32] in order to achieve quantitative results. There have been several reports on the application of these improved procedures to materials subjected to ECAP, and it is instructive to compare the present results with those reported in these other investigations. The other reports divide into two categories, for samples of pure copper[33–36] and for aluminum alloys,[17,37,38] respectively. These two materials are now considered separately.

The most comprehensive report for copper relates to a sample pressed for eight passes through a 90 deg die using route B_C.[36] By taking careful measurements of the individual boundary orientations using the Kikuchi patterns, it was concluded that high-angle disorientations developed along extended boundaries separating bands or groups of bands of subgrains. This led to the conclusion that the substructure developed by ECAP of pure copper was not strictly an ultrafine grain structure, but rather it was characteristic of well-established deformation structures observed in heavily rolled materials where boundaries having high disorientation angles separate an essentially lamellar structure.[39] It was also reported that the fraction of high-angle boundaries present in the pure copper after ECAP was ~37 pct. This is lower than would be the case for the material of the current study at the same processing strain. Interpolation of the results for four and 12 passes in the data in Figure 13 suggest that ~60 to ~75 pct of the boundaries would be high-angle in nature. Furthermore, such a structure would be fully homogeneous. Since the apparent grain sizes obtained by TEM and OIM for a material after four and 12 passes were

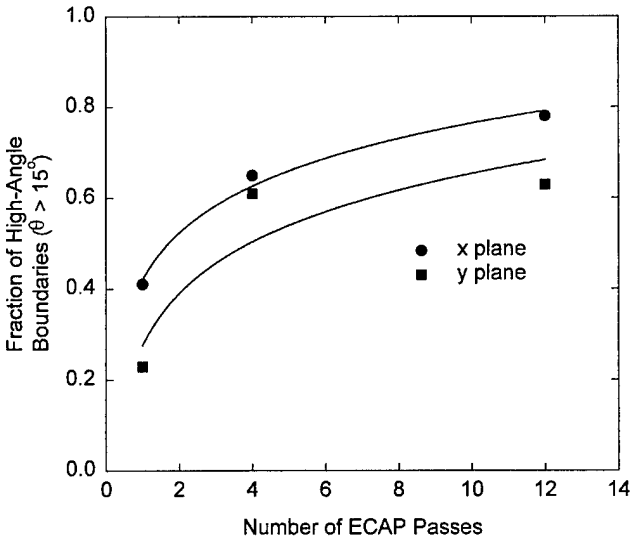

Fig. 13—The fraction of high-angle boundaries (disorientation > 15 deg) as a function of the number of ECAP passes, N_p, for pure aluminum processed by route B_C for repetitive pressing. Data are included for both the x and y planes of the samples examined. Repetitive pressing results in a progressive increase in the fraction of high-angle boundaries. The fraction of high-angle boundaries is always greater on the x plane.

essentially the same, it is unlikely that such apparent differences are due to incomplete sampling in the aluminum data. The difference may be attributed instead to the low stacking-fault energy of copper and consequent low rate of recovery, which leads, as noted in an earlier study of ECAP of copper,[40] to an inability to attain a fully homogeneous structure during the pressing of pure copper even after a total of 10 passes through the die. In this respect, the data of Mishin, *et al.*[36] were obtained for a sample pressed through only eight passes.

There are several reports on the application of EBSD methods to aluminum alloys after processing by ECAP,[37,38] but unfortunately, these results refer almost exclusively to samples pressed through a die having an internal angle of 120 deg. It is difficult to interpret these results for two reasons. First, it is now well established that an internal angle of 90 deg is needed in order to most readily establish an array of equiaxed and ultrafine grains separated by high-angle boundaries.[41] Second, there is an important difference between results anticipated using dies with angles of 90 and 120 deg, because of an apparent interaction between the shear plane and the texture formed during ECAP in the die with the higher angle.[42]

In summary, the present results provide a detailed initial report on the application of EBSD/OIM methods after ECAP of pure aluminum, a material wherein it appears to be relatively easy to attain a uniform, essentially equiaxed grain structure and a high population of high-angle boundaries. These results confirm that ECAP is effective, at least for pure aluminum, in producing exceptional grain refinement and a large fraction of high-angle boundaries. In practice, high-angle boundaries are needed to achieve grain-boundary sliding in superplastic deformation, and the present results are consistent with reports of very high tensile ductilities (up to ~2000 pct elongation) in aluminum alloys after processing by ECAP.[43,44]

V. CONCLUSIONS

1. For pure aluminum of an initial grain size of 1 mm, TEM reveals elongated bands of subgrains following an initial ECAP pass through a 90 deg die. Corresponding OIM investigations reveal that the microstructure and microtexture are not homogeneous, although the distributions of grain-to-grain disorientations also indicate a predominance of subgrains in this material. Grain maps and the disorientation data depend on the plane of examination and are not isotropic.
2. Repetitive ECAP by route B_C results in homogenization of the microstructure and microtexture. After four ECAP passes, nearly equiaxed grains, 1.2 μm in size, remain aligned with the shear direction of the fourth pressing operation, and these grains appear to be organized into bands aligned with the shear direction on the shear plane. While the texture still varies with location, a $\langle 111 \rangle$ orientation tends to align with the shear direction. The disorientation data clearly indicate an upward shift in the distributions, which reflects recovery-controlled accumulation of dislocations into the boundaries. Different disorientation distributions are obtained on the y and x planes, and this reflects the presence of bands in the structure.
3. Following 12 ECAP passes by route B_C, the grain size decreases slightly to about 1.0 μm. A B-type shear texture developed during ECAP passes beyond the fourth pressing pass by route B_C. The influence of billet rotation between successive passes in route B_C on shear-texture development during repetitive ECAP has not been determined and should be the subject of further investigation. The disorientation distributions indicate a further upward shift in boundary disorientation and a predominance of high-angle boundaries in the microstructure. After 12 ECAP passes, ~63 pct (y plane) to ~78 pct (x plane) of the boundaries are high-angle in nature, although the distribution remains anisotropic in nature.

ACKNOWLEDGMENTS

We thank Dr. Y. Li for experimental assistance in the early stages of this investigation and Professor M. Nemoto for encouragement. Support for this work was provided by the Light Metals Educational Foundation of Japan, the United States Office of Naval Research–Asia, and the United States Army Research Office under Grant No. DAAD19-00-1-0488.

REFERENCES

1. R.Z. Valiev, R.R. Mulyukov, V.V. Ovchinnikov, and V.A. Shabashov: *Scripta Metall. Mater.*, 1991, vol. 25, pp. 2717-22.
2. N.A. Akhmadeev, V.I. Kopylov, R.R. Mulyukov, and R.Z. Valiev: *Izv. Akad. Nauk SSSR Met.*, 1992, vol. 5, pp. 91-101.
3. J. Wang, Z. Horita, M. Furukawa, M. Nemoto, N.K. Tsenev, R.Z. Valiev, Y. Ma, and T.G. Langdon: *J. Mater. Res.*, 1993, vol. 8, pp. 2810-18.
4. T.G. Langdon, M. Furukawa, M. Nemoto, and Z. Horita: *JOM*, 2000, vol. 52 (4), pp. 30-33.
5. R.Z. Valiev, O.A. Kaibyshev, R.I. Kuznetsov, R.S. Musalimov, and N.K. Tsenev: *Dokl. Akad. Nauk SSSR* 1988, vol. 301, pp. 864-66.
6. O.A. Kaibyshev, R. Kaibyshev, and G. Salishchev: *Mater. Sci. Forum*, 1993, vols. 113–115, pp. 423-28.

7. G.A. Salishchev, R.M. Imayev, V.M. Imayev, and N.K. Gabdullin: *Mater. Sci. Forum*, 1993, vols. 113–115, pp. 613-18.
8. R.Z. Valiev, N.A. Krasilnikov, and N.K. Tsenev: *Mater. Sci. Eng.*, 1991, vol. A137, pp. 35-40.
9. C.C. Koch and Y.S. Cho: *Nanostruct. Mater.*, 1992, vol. 1, pp. 207-12.
10. D.A. Rigney: *Ann. Rev. Mater. Sci.*, 1988, vol. 18, pp. 141-63.
11. J. Wang, Z. Horita, M. Furukawa, M. Nemoto, R.Z. Valiev, and T.G. Langdon: *Mater. Sci. Eng.*, 1996, vol. A216, pp. 41-46.
12. M. Furukawa, Z. Horita, M. Nemoto, R.Z. Valiev, and T.G. Langdon: *Acta Mater.*, 1996 vol. 44, pp. 4619-29.
13. Y. Iwahashi, Z. Horita, M. Nemoto, and T.G. Langdon: *Acta Mater.*, 1998, vol. 46, pp. 3317-31.
14. Z. Horita, T. Fujinami, M. Nemoto, and T.G. Langdon: *Metall. Mater. Trans. A*, 2000, vol. 31A, pp. 691-701.
15. V.M. Segal: *Mater. Sci. Eng.*, 1995, vol. A197, pp. 157-64.
16. Y. Iwahashi, Z. Horita, M. Nemoto, and T.G. Langdon: *Acta Matter.*, 1997, vol. 45, pp. 4733-41.
17. A. Gholinia, P.B. Prangnell, and M.V. Markushev: *Acta Mater.*, 2000, vol. 48, pp. 1115-30.
18. M. Furukawa, Y. Iwahashi, Z. Horita, M.. Nemoto, and T.G. Langdon: *Mater. Sci. Eng.*, 1998, vol. A257, pp. 328-32.
19. K. Oh-ishi, Z. Horita, M. Furukawa, M. Nemoto, and T.G. Langdon: *Metall. Mater. Trans. A*, 1998, vol. 29A, pp. 2011-13.
20. S.D. Terhune, Z. Horita, M. Nemoto, Y. Li, T.G. Langdon, and T.R. McNelley: *Proc ReX'99*, 4th Int. Conf. on Recrystallization and Related Phenomena, T. Sakai and H.G. Suzuki, eds., Japan Institute of Metals, Sendai, Japan, 1999, pp. 515-22.
21. S.C. Vogel: Los Alamos National Laboratory, Los Alamos, NM, private communication, 2002
22. Y. Iwahashi, J. Wang, Z. Horita, M. Nemoto, and T.G. Langdon: *Scripta Mater.*, 1996, vol. 35, pp. 143-46.
23. J.R. Bowen, A. Gholinia, S.M. Roberts, and P.B. Prangnell: *Mater. Sci. Eng.*, 2000, vol. A287, pp. 87-99.
24. H.S. Kim, M.H. Seo, and S.I. Hong: *Mater Sci. Eng.*, 2000, vol. A291, pp. 86-90.
25. D. Yamaguchi, Z. Horita, M. Nemoto, and T.G. Langdon: *Scripta Mater.*, 1999, vol. 41, pp. 791-96.
26. V. Randle: *Microtexture Determination and Its Applications*, The Institute of Metals, London, 1992.
27. G.R. Canova, U.F. Kocks, and J.J. Jonas: *Acta Metall.*, 1984, vol. 32, pp. 211-26.
28. C.P. Chang, P.L. Sun, and P.W. Kao: *Acta Mater.*, 2000, vol. 48, pp. 3377-85.
29. J.Y. Chang, J.S. Yoon, and G.H. Kim: *Scripta Mater*, 2001, vol. 45, pp. 347-54.
30. J.K. Mackenzie: *Biometrika*, 1958, vol. 45, pp. 229-40.
31. M.T. Pérez-Prado and T.R. McNelley: *Scripta Mater.*, 1999, vol. 40, pp. 1401-06.
32. Q. Liu: *Ultramicroscopy*, 1995, vol. 60 pp. 81-89.
33. O.V. Mishin, V.Y. Gertsman, R.Z. Valliev, and G. Gottstein: *Scripta Mater.*, 1996, vol. 35, pp. 873-78.
34. S.R. Agnew, U.F. Kocks, K.T. Hartwig, and J.R. Weertman: in *Modeling of Structure and Mechanics of Materials from Microscale to Product*, J.V. Carstensen, T. Leffers, T. Lorentzen, O.B. Pedersen, B.F. Sørensen, and G. Winther, eds. Risø National Laboratory, Roskilde, Denmark, 1998, pp. 201-06.
35. D.P. Field and H. Weiland: in *Electron Backscatter Diffraction in Materials Science*, A.J. Schwartz, M. Kumar, and B.L. Adams, eds., Kluwer Academic Press, New York, NY, 2000, pp. 199-212.
36. O.V. Mishin, D. Juul Jensen, and N. Hansen: in *Recrystallization—Fundamental Aspects and Relations to Deformation Microstructure*, N. Hansen, X. Huang, D. Juul Jensen, E.M. Lauridsen, T. Leffers, W. Pantleon, T. Sabin, and J.A. Wert, eds. Risø National Laboratory, Roskilde, Denmark, 2000, pp. 445-48.
37. P.B. Prangnell, J.R. Bowen, A. Gholinia, and M.V. Markushev: *Materials Research Society Symposium Proceedings*, Materials Research Society, Pittsburgh, PA, 2000, vol. 601, pp. 323-34.
38. P.B. Prangnell, A. Gholinia, and M.V. Markushev: in *Investigations and Applications of Severe Plastic Deformation*, T.C. Lowe and R.Z. Valiev, eds., Kluwer Academic, Dordrecht, The Netherlands, 2000, pp. 65-71.
39. D.A. Hughes and N. Hansen: *Acta Mater.*, 1997, vol. 45, pp. 3871-86.
40. S. Komura, Z. Horita, M. Nemoto, and T.G. Langdon: *J. Mater Res.*, 1999, vol. 14, pp. 4044-50.
41. K. Nakashima, Z. Horita, M. Nemoto, and T.G. Langdon: *Acta Mater.*, 1998, vol. 46, pp. 1589-99.
42. Y.T. Zhu and T.C. Lowe: *Mater. Sci. Eng.*, 2000, vol. A291, pp. 46-53.
43. Z. Horita, M. Furukawa, M. Nemoto, A.J. Barnes, and T.G. Langdon: *Acta Mater.*, 2000, vol. 48, pp. 3633-40.
44. S. Komura, Z. Horita, M. Furukawa, M. Nemoto, and T.G. Langdon: *Metall. Mater. Trans. A.*, 2001, vol. 32A, pp. 707-16.